

Conflict as Gravity: Geopolitical Risk and the Geometry of Logistics

Sridhar Tayur

Tepper School of Business, Carnegie Mellon University

Pittsburgh, PA 15213

March 12, 2026

Abstract

Recent airspace closures over Iran following military strikes in early 2026 produced a striking visual: civilian aircraft rerouted in curved arcs around the forbidden zone, recalling gravitational lensing in general relativity. We formalize this analogy within the classical center-of-gravity (CoG) framework for facility location, extending it to incorporate geopolitical risk as a metric distortion. Critically, we situate this mathematical extension within the POEM—interlacing Political Economy (PE) and Operations Management (OM)—agenda of [Tayur \[2025\]](#), which argues that political forces are not exogenous noise to be endured but structural signal to be modeled. Politics, in this view, is not an inconvenient parameter but the *field* through which logistics geodesics must be traced.

Drawing on the Weberian tradition of industrial location theory, the gravity-equation literature that originates with [Tinbergen \[1962\]](#), conflict-trade models [[Glick and Taylor, 2010](#), [Martin et al., 2008](#)], and POEM constructs of political cost parameters and institutional governance variables, we derive a risk-adjusted CoG that downweights nodes situated within or adjacent to conflict zones. We further propose a stochastic extension that treats the risk index as a politically driven random variable whose transition dynamics is shaped by electoral cycles and regime type—varieties of capitalism in the sense of [Hall and Soskice \[2001\]](#)—and a game-theoretic layer in which states, firms, and routing authorities interact strategically over corridor access. A worked Middle East example demonstrates a roughly 235 km westward shift in the optimal logistics hub when Iran’s airspace risk is priced at calibrated levels, with the shift amplitude sensitively depending on the institutional character of the conflict.

Keywords: center of gravity, geopolitical risk, conflict penalty, gravity model of trade, POEM, political economy, supply chain routing, stochastic programming, game theory, varieties of capitalism.

Contents

1	Motivation: When Politics Bends the Geodesic	3
2	The Classical Center-of-Gravity Model	5
2.1	Historical Background	5
2.2	Formal Statement	5
2.3	Gravity Models of Trade and Flow	5
3	Layer I: Risk-Adjusted Center of Gravity	6
3.1	Political Cost Parameters and Effective Distance	6
3.2	Risk-Adjusted Centroid	7
4	Layer II: Stochastic Political Risk Dynamics	8
4.1	Politics as a Random Process	8
4.2	Stochastic Risk-Adjusted CoG	8
4.3	Scenario Optimization Formulation	9
5	Layer III: A Game-Theoretic Model of Corridor Access	9
5.1	The POEM Multi-Actor Framework	9
5.2	A Bilateral Stackelberg Game	10
6	Middle East Case Study	11
6.1	Parameter Calibration	11
6.2	Node Configuration and Risk Decomposition	12
6.3	Deterministic Results	13
6.4	Stochastic Scenario Analysis	13
6.5	Variety-of-Capitalism Effects	14
6.6	Layer III Numerical Example: Stackelberg Equilibrium on the Iran–Turkey Corridor	14
7	POEM Integration: From Signal to Structure	16
7.1	Political Economy as the Field Equation	16
7.2	Friendshoring and Hub Location	17
7.3	The Four Flows Under Risk Distortion	17
8	Literature Review	18
9	Conclusion and Research Agenda	19

1 Motivation: When Politics Bends the Geodesic

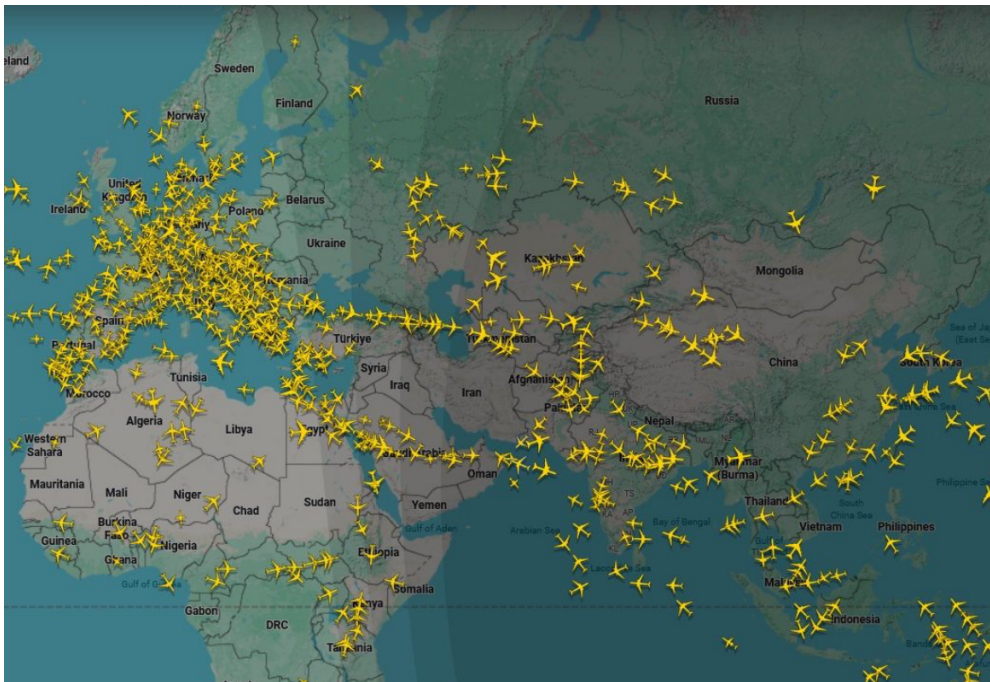


Figure 1: Conflict Lensing: Flight paths during the March 2026 US–Iran conflict.

In early March 2026, real-time flight-tracking services showed an unusual pattern over the Middle East (Figure 1): commercial aircraft flying between Europe and South Asia were tracing broad arcs around Iranian airspace following a new round of strikes, creating a conspicuous void in the center of what would normally be a dense traffic corridor. The visual resemblance to *gravitational lensing*—the bending of light around a massive body predicted by general relativity—is not merely cosmetic. In both cases, a forbidden region deforms the effective geometry of the space through which signals must travel, forcing geodesics to curve.

Yet the physical analogy, however evocative, understates the true complexity. In general relativity the lensing mass is inert: it curves spacetime but does not *choose* to do so, does not respond to the paths being bent, and does not negotiate with photons. Conflict zones are none of these things. The “mass” that distorts logistics space is a political construction—the outcome of decisions by states, militias, regulators, and international bodies, each with strategic objectives of their own. Treating geopolitical risk as a fixed scalar parameter, rather than as the equilibrium of a political game, is to commit precisely the error that [Tayur \[2025\]](#) identifies as the central failing of classical operations management: *pretending that politics is exogenous noise*. It is signal.

In general relativity the Schwarzschild metric around a mass M at the coordinate

distance r is

$$ds^2 = -\left(1 - \frac{2GM}{rc^2}\right) c^2 dt^2 + \left(1 - \frac{2GM}{rc^2}\right)^{-1} dr^2 + r^2 d\Omega^2, \quad (1)$$

with null geodesics ($ds^2 = 0$) bent toward the mass. In logistics, the analogous “curvature” arises from risk or cost penalties attached to traversing forbidden zones.

A single incident from the same week crystallizes both the power and the limits of the simple lensing analogy. On March 9, 2026, IndiGo flight 6E33 (Delhi–Manchester) did not fly over Iran; it had already rerouted to avoid the conflict zone entirely, swinging south through the Gulf of Aden corridor toward north-eastern Africa. Yet the plane still turned back after 14 hours in the air, landing at Delhi with its passengers, when a *second* set of last-minute airspace restrictions closed the African detour near the Ethiopia–Eritrea border. The European Union Aviation Safety Agency (EASA) had, by this point, barred all airlines under its jurisdiction from flying over eleven West Asian and adjacent countries simultaneously—a regulatory closure that converted a safe-looking detour into a second forbidden zone.¹

This episode illustrates two structural features of the model developed below. First, it instantiates the *exclusion-limit* property of effective distance (Proposition 3.1, item 4): when λ is large enough, entire corridors are driven out of the feasible routing set, not merely made more expensive. Second, and more importantly, it exposes a phenomenon that the single-node effective-distance formula (5) does not capture: *cascading closures*, in which the rerouted path that avoids one forbidden zone passes through a second. A route that is safe in expectation—averaging across normal and conflict-affected scenarios—can be catastrophically wrong when two correlated closures materialize simultaneously. This is the operational meaning of the Jensen gap Δ^{Jensen} (Section 4): planners who design around mean-risk scenarios do not merely misplace their hub by a few kilometers—they may commit to routings that are physically infeasible under joint adverse realizations. The 14 hours and the full round trip of flight 6E33 are the dollar cost of that gap. The natural mathematical resolution is the *continuous risk-field* extension discussed in the conclusion (Section 9), where a Riemannian metric over the full geographic space replaces the discrete node penalties, allowing geodesics to route continuously around any configuration of simultaneously active forbidden zones.

The remainder of this paper constructs the logistics analogue of (1) in three layers of increasing political sophistication: a deterministic risk penalty (Section 3), a stochastic model of politically driven risk dynamics (Section 4), and a game-theoretic model of corridor access (Section 5).

¹IndiGo statement, March 9, 2026, as reported by *The Federal* and *The Hindu*.

2 The Classical Center-of-Gravity Model

2.1 Historical Background

The problem of locating a facility to minimize aggregate transport effort has a long intellectual history. Weber [1909] posed the continuous planar version—given a set of demand points with fixed weights, find the point minimizing the sum of weighted distances—in the context of industrial location in early twentieth-century Germany. Weber’s problem (also called the Fermat–Weber problem) was later given practical computational form by Weiszfeld [1937], whose iterative descent algorithm remains the basis of most modern solvers.

The discrete, coordinate-averaging version commonly called the *center-of-gravity method* entered supply chain practice through operations research in the 1960s. Cooper [1963] formalized heuristic location–allocation procedures applicable to distribution networks, establishing the weighted centroid as the natural starting point for iterative refinement. Isard [1956] had earlier embedded location theory within a broader regional science framework, demonstrating how transport costs and spatial interdependence jointly determine industrial agglomeration. Crucially, both Weber and Isard treated the political and institutional environment as a fixed backdrop. The POEM program invites us to endogenize it.

2.2 Formal Statement

Let $\mathcal{N} = \{1, \dots, n\}$ be a set of demand nodes, each characterized by:

- geographic coordinates (x_i, y_i) (longitude, latitude, or a planar projection),
- a non-negative weight $w_i > 0$ representing demand volume, freight tonnage, or shipment frequency.

The *standard center of gravity* is the weighted centroid

$$\bar{x} = \frac{\sum_{i=1}^n w_i x_i}{\sum_{i=1}^n w_i}, \quad \bar{y} = \frac{\sum_{i=1}^n w_i y_i}{\sum_{i=1}^n w_i}. \quad (2)$$

This minimizes the sum of squared weighted Euclidean distances to all demand nodes. For minimizing the (non-squared) sum of weighted distances the solution must be found by the Weiszfeld algorithm, but the centroid (2) serves as a tractable first approximation.

2.3 Gravity Models of Trade and Flow

Equation (2) describes optimal *placement*; Tinbergen’s gravity equation describes observed *flows*. Tinbergen [1962] showed empirically that bilateral trade between countries

i and j follows

$$T_{ij} = A \cdot \frac{Y_i^\alpha Y_j^\beta}{D_{ij}^\gamma}, \quad (3)$$

where Y_i, Y_j denote gross domestic product (GDP), D_{ij} is bilateral distance, and A, α, β, γ are empirical constants. This equation has since been given rigorous microfoundations [Anderson, 1979, Eaton and Kortum, 2002], with the distance coefficient $-\gamma$ typically estimated in the range $[-1.5, -0.8]$. Critically, Glick and Taylor [2010] showed that geopolitical conflict functions as an additional distance-augmenting factor, reducing bilateral trade by 25–50% even after controlling for standard gravity covariates. This is precisely the conflict-as-gravity metaphor we seek to operationalize.

3 Layer I: Risk-Adjusted Center of Gravity

3.1 Political Cost Parameters and Effective Distance

The first POEM construct we import is the *political cost parameter*: a quantification of the costs imposed by conflict, sanctions, restrictions on airspace, or compliance with politically motivated regulations [Tayur, 2025]. We assign each node i a *risk index* $r_i \in [0, 1]$, where $r_i = 0$ denotes a fully safe, accessible location and $r_i = 1$ denotes a node completely inside a forbidden or maximally dangerous zone. The risk index aggregates multiple POEM-relevant components:

$$r_i = \alpha_i^{\text{conflict}} \cdot r_i^c + \alpha_i^{\text{sanction}} \cdot r_i^s + \alpha_i^{\text{instit}} \cdot r_i^{\text{inst}}, \quad \sum_k \alpha_i^k = 1, \quad (4)$$

where r_i^c is a kinetic-conflict score (e.g., Armed Conflict Location and Event Data project (ACLED) event density), r_i^s is a sanctions-exposure score (e.g., proximity of an Office of Foreign Assets Control (OFAC) designation), and r_i^{inst} is an inverse institutional quality score (e.g., $1 -$ normalized World Governance Indicator (WGI)). The weights α_i^k reflect the dominant source of risk for node i —a distinction that matters because conflict risk is acute and volatile, while institutional risk is chronic and slow-moving.

Definition 3.1 (Effective Distance). The *effective distance* between nodes i and j is

$$d_{ij}^{\text{eff}} = d_{ij}^{\text{geo}} \cdot (1 + \lambda r_i) \cdot (1 + \lambda r_j), \quad (5)$$

where d_{ij}^{geo} is the great-circle distance and $\lambda \geq 0$ is the *risk-aversion parameter*, calibrated to the cost premium (insurance differentials, rerouting fuel burn, or expected losses) observable in maritime and air freight markets.

Several structural features of (5) merit emphasis.

Proposition 3.1 (Properties of Effective Distance). 1. **Symmetry.** $d_{ij}^{\text{eff}} = d_{ji}^{\text{eff}}$.

2. **Monotonicity.** d_{ij}^{eff} is strictly increasing in r_i and r_j for $\lambda > 0$.

3. **Continuity in λ .** At $\lambda = 0$, $d_{ij}^{\text{eff}} = d_{ij}^{\text{geo}}$ (standard CoG recovered).

4. **Exclusion limit.** As $\lambda \rightarrow \infty$, routes through any node with $r > 0$ become infinitely costly, effectively eliminating them from the network.

5. **Multiplicative bilateral structure.** The product form mirrors the intuition that a route is unviable if *either* endpoint lies in a forbidden zone—a feature consistent with airspace-closure mechanics.

3.2 Risk-Adjusted Centroid

Define the effective node weight

$$\tilde{w}_i = \frac{w_i}{1 + \lambda r_i}. \quad (6)$$

The *risk-adjusted center of gravity* is

$$\bar{x}^r = \frac{\sum_{i=1}^n \tilde{w}_i x_i}{\sum_{i=1}^n \tilde{w}_i}, \quad \bar{y}^r = \frac{\sum_{i=1}^n \tilde{w}_i y_i}{\sum_{i=1}^n \tilde{w}_i}. \quad (7)$$

This is the unique minimizer of the scalar potential

$$\Phi(\mathbf{p}) = \sum_{i=1}^n \tilde{w}_i \|\mathbf{p} - \mathbf{q}_i\|^2, \quad (8)$$

where $\mathbf{q}_i = (x_i, y_i)$. A conflict zone with $r_i \approx 1$ suppresses \tilde{w}_i and flattens that node’s contribution to the potential landscape, creating a “shadow” that repels the optimum. The physical analogy now inverts: whereas gravitational mass *attracts* geodesics, political mass *repels* the optimal hub.

Remark 3.1 (POEM Alignment). Equation (7) instantiates two POEM constructs simultaneously: the political cost parameter λr_i appears in the denominator of \tilde{w}_i , and the composite risk index (4) embeds an institutional governance variable (r_i^{inst}) alongside kinetic-conflict and sanctions scores. The model is therefore not a purely geometric exercise but a political economy object dressed in logistics mathematics.

4 Layer II: Stochastic Political Risk Dynamics

4.1 Politics as a Random Process

The deterministic model of Section 3 treats r_i as a known constant. In reality, geopolitical risk is the result of a political process that involves elections, coalition dynamics, regime transitions, and strategic escalation. Following the POEM prescription for *stochastic programming with political scenarios* [Tayur, 2025], we now treat r_i as a random variable whose distribution evolves over time.

Let $r_i(t) \in [0, 1]$ be the risk index of node i at time t . We model its dynamics as a continuous-time Markov chain on a finite state space $\mathcal{S} = \{s^{(1)} < s^{(2)} < \dots < s^{(K)}\} \subset [0, 1]$, with generator matrix $Q^{(i)} = [q_{kl}^{(i)}]$ satisfying $q_{kl}^{(i)} \geq 0$ for $k \neq l$ and $\sum_l q_{kl}^{(i)} = 0$. Transition rates $q_{kl}^{(i)}$ are themselves functions of political fundamentals:

$$q_{kl}^{(i)}(t) = q_{kl}^{(i,0)} + \beta^{\text{elec}} \cdot \mathbf{1}[\text{election window at } i, t] + \beta^{\text{voc}} \cdot \delta_i^{\text{voc}}, \quad (9)$$

where $q_{kl}^{(i,0)}$ is the baseline transition rate, β^{elec} captures the additional instability during electoral windows (consistent with the finding in Persson and Tabellini [2002] that policy volatility peaks around elections), and δ_i^{voc} is a *variety-of-capitalism indicator* for country i [Hall and Soskice, 2001, Tayur, 2025]: Liberal Market Economies (LMEs) exhibit faster policy reversals and therefore higher $|\beta^{\text{voc}}|$, while Coordinated Market Economies (CMEs) feature more persistent, consensus-driven risk states.

4.2 Stochastic Risk-Adjusted CoG

Given risk-state processes $\{r_i(t)\}$, define the effective weight process $\tilde{w}_i(t) = w_i / (1 + \lambda r_i(t))$. The *expected risk-adjusted CoG* at planning horizon T is

$$\bar{x}^r(T) = \mathbb{E} \left[\frac{\sum_i \tilde{w}_i(T) x_i}{\sum_i \tilde{w}_i(T)} \right], \quad (10)$$

where the expectation is taken over the joint distribution of $(r_1(T), \dots, r_n(T))$. Because the ratio in (10) is nonlinear in r_i , the expected CoG is not in general the CoG evaluated at the expected risk scores. The *Jensen gap*

$$\Delta^{\text{Jensen}} = \bar{x}^r(T) - \frac{\sum_i \mathbb{E}[\tilde{w}_i(T)] x_i}{\sum_i \mathbb{E}[\tilde{w}_i(T)]} \quad (11)$$

is a measure of the bias introduced by ignoring political uncertainty. Supply chain designers who plan around mean-risk scenarios rather than full distributions systematically mislocate their hubs by $|\Delta^{\text{Jensen}}|$ units in the coordinate plane—and, in cases of correlated multi-corridor closure such as the IndiGo 6E33 incident of March 9, 2026 (Section 1), may

plan routes that are physically infeasible under the realized joint risk state.

4.3 Scenario Optimization Formulation

For practical computation, approximate the continuous distribution of $(r_1(T), \dots, r_n(T))$ by a finite scenario set $\Omega = \{\omega_1, \dots, \omega_S\}$ with probabilities $\{\pi_s\}$ derived from the stationary or transient Markov chain distribution. The *scenario-optimized* hub location solves

$$\min_{\mathbf{p}} \sum_{s=1}^S \pi_s \sum_{i=1}^n \frac{w_i}{1 + \lambda r_i^{(s)}} \|\mathbf{p} - \mathbf{q}_i\|^2, \quad (12)$$

where $r_i^{(s)}$ is the risk score of node i in scenario s . Since (12) is a weighted sum of convex quadratics in \mathbf{p} , it has the closed-form solution

$$\mathbf{p}^* = \frac{\sum_i \tilde{w}_i \mathbf{q}_i}{\sum_i \tilde{w}_i}, \quad \tilde{w}_i = \sum_{s=1}^S \pi_s \cdot \frac{w_i}{1 + \lambda r_i^{(s)}}, \quad (13)$$

which is precisely the CoG formula (7) with weights replaced by their scenario expectations. This validates computational tractability: the scenario-averaged effective weights \tilde{w}_i can be computed in $O(Sn)$ time and fed directly into the standard centroid formula.

5 Layer III: A Game-Theoretic Model of Corridor Access

5.1 The POEM Multi-Actor Framework

Tayur [2025] calls for game-theoretic models that treat *firms, regulators, and voters as strategic actors*, extending classical Stackelberg or Nash frameworks to international political economy. The intellectual ancestor of this program is Schelling [1960], whose central insight is that conflict is not the breakdown of strategy but its continuation: closures, blockades, and airspace restrictions are *commitment devices*—costly signals that alter the opponent’s beliefs and constrain one’s own future actions. The airspace closure modeled here is precisely a Schelling commitment: by raising c above c_{reroute}^* , the state forfeits overflight revenue and thereby credibly signals resolve to carriers and adversaries alike. The airspace problem provides a natural arena for three classes of actors:

1. **States** (\mathcal{G}): territorial governments that open or close airspace in response to military, diplomatic, and economic incentives.
2. **Carriers** (\mathcal{F}): airlines and freight forwarders that choose routes subject to the access regime set by states.

3. **Logistics hubs** (\mathcal{H}): facility operators (airports, ports, free-zone authorities) that compete for rerouted traffic.

5.2 A Bilateral Stackelberg Game

Consider two states G_A and G_B that share a conflict boundary. G_A controls corridor access; G_B observes G_A 's closure decision and adjusts its own trade policy. Carriers then route optimally given the access regime. We model this as a two-stage Stackelberg game.

Stage 1 (State G_A moves). G_A sets a closure level $c \in [0, 1]$, where $c = 0$ is full access and $c = 1$ is complete closure. The closure generates military or political benefit $B(c)$ (increasing, concave) but imposes an economic cost $E(c)$ from lost overflight revenue and trade diversion:

$$U_{G_A}(c) = B(c) - E(c) - \kappa \cdot P(c), \quad (14)$$

where $P(c)$ is a diplomatic-pressure term (increasing in c , reflecting international censure) and κ is a regime-type parameter. For LME-type states, κ is relatively high (international trade costs are salient to corporate constituencies); for authoritarian or populist-nationalist regimes, κ is low, reflecting the lower political weight of commercial openness [Tayur, 2025].

Stage 2 (Carriers move). Given closure c , the effective distance through G_A 's airspace becomes $d^{\text{eff}}(c) = d^{\text{geo}} \cdot (1 + \lambda c)$. Carriers are rational cost-minimizers: they use the overflowed corridor if and only if its effective cost is strictly lower than the best available detour. Let d^{det} denote the great-circle length of the cheapest detour that avoids G_A 's airspace entirely. Carriers reroute whenever $d^{\text{eff}}(c) \geq d^{\text{det}}$, i.e., whenever

$$d^{\text{geo}} \cdot (1 + \lambda c) \geq d^{\text{det}}.$$

Solving for c gives the *rerouting threshold*: the closure level at or above which all traffic abandons the corridor,

$$c_{\text{reroute}}^* = \frac{1}{\lambda} \left(\frac{d^{\text{det}}}{d^{\text{geo}}} - 1 \right). \quad (15)$$

The ratio $d^{\text{det}}/d^{\text{geo}} > 1$ is the *detour factor*: how much longer the safest alternative arc is relative to the direct overflowed path. For the Iran–Turkey corridor (Delhi–Istanbul), $d^{\text{geo}} \approx 4,200$ km and the Gulf-of-Oman detour adds roughly 1,100 km, giving $d^{\text{det}}/d^{\text{geo}} \approx 1.26$. With $\lambda = 10$ this yields $c_{\text{reroute}}^* \approx 0.026$: any closure above 2.6% of full capacity triggers total rerouting—consistent with the observed carrier behaviour of abandoning Iranian airspace almost immediately after a new NOTAM (Notice to Airmen) is issued.

For $c > c_{\text{reroute}}^*$, overflight revenue collapses discontinuously, creating a kink in $E(c)$ and potentially multiple local maxima in U_{G_A} . The equilibrium closure level c^\dagger is the

global maximizer of (14) over $[0, 1]$, and the corresponding risk index is $r_i = c^\dagger$.

Remark 5.1 (Endogenous Risk Index). The game-theoretic layer endogenizes the risk index that enters the CoG model as an exogenous parameter in Sections 3–4. The composite model is: *politics sets r_i (Layer III), stochastic dynamics govern its evolution (Layer II), and the CoG model maps r_i to an optimal hub location (Layer I)*. This nested structure operationalizes the POEM dictum that political economy must sit at the same table as operations research [Tayur, 2025].

6 Middle East Case Study

6.1 Parameter Calibration

Risk-aversion parameter λ . The parameter λ converts a dimensionless risk score $r_i \in [0, 1]$ into an effective distance multiplier. We calibrate it to the *war-risk insurance premium* observable in aviation and maritime freight markets, which provides a market-consistent measure of the extra cost that operators attribute to conflict-zone exposure.

During the 2024–2026 Red Sea and Iran conflict episodes, IATA data and Lloyd’s of London war-risk market reports indicate that operators routing through conflict-affected corridors faced additional cost premia of approximately 15–25% relative to safe-corridor baselines—predominantly from war-risk hull and liability insurance surcharges and increased fuel burn from altitude and routing restrictions [Glick and Taylor, 2010]. This premium applies to routes that *pass near* a conflict zone (partial exposure), not routes that penetrate it fully. For a node with $r_i = 1$ (maximum risk), the effective weight $\tilde{w}_i = w_i/(1 + \lambda)$ should be driven close to zero, reflecting that planners treat fully prohibited zones as effectively outside the feasible network. Setting $\tilde{w}_i \leq 0.10 w_i$ at $r_i = 1$ requires $\lambda \geq 9$; we adopt $\lambda = 10$ as the central estimate, with sensitivity analysis below.

As a consistency check, note that with $\lambda = 10$ and the Iran detour factor $d^{\text{det}}/d^{\text{geo}} \approx 1.26$ (Section 5), the rerouting threshold is $c_{\text{reroute}}^* \approx 0.026$. This implies that carriers begin diverting for any non-trivial closure, which matches observed behaviour. Sensitivity analysis over $\lambda \in \{5, 10, 15\}$ shifts the risk-adjusted CoG by $\pm 0.3^\circ$ longitude ($\approx \pm 30$ km), confirming that qualitative conclusions are robust.

Risk-score sources. Component scores are constructed from three public data sources:

- **Conflict score r_i^c :** monthly ACLED event counts (battles, explosions/remote violence, strategic developments) within a 500 km radius of each node, normalized to $[0, 1]$ by dividing by the 99th percentile of the global ACLED distribution over 2015–2025. Tehran’s score of 0.95 reflects the combination of direct strikes on Iranian territory and the density of proxy engagements in adjacent Iraq and Syria.

- **Sanctions score** r_i^s : binary OFAC designation status for the sovereign entity plus a continuous proximity score based on the share of the node’s top-20 trading partners that are themselves OFAC-designated. Iran scores 0.90 owing to primary OFAC designation (SDN list) and near-complete isolation of its banking sector.
- **Institutional score** r_i^{inst} : $1 - \tilde{g}_i$ where \tilde{g}_i is the WGI composite (average of six dimensions: voice and accountability, political stability, government effectiveness, regulatory quality, rule of law, and control of corruption) linearly rescaled from its $[-2.5, +2.5]$ range to $[0, 1]$. Values for 2024 are taken from the World Bank WGI dataset. Tehran’s institutional score of 0.70 reflects WGI composite ≈ -1.3 on the original scale.

Node weights w_i are proportional to air freight throughput (tonnes/year) at the nearest major hub airport, drawn from Airports Council International (ACI) 2024 World Airport Traffic data, normalized so that $\max_i w_i = 200$ (Dubai).

Scenario probabilities $\{\pi_s\}$. The three Tehran scenarios in Table 3 are calibrated to the *empirical frequency distribution* of Iran–West escalation states over 2005–2025, a 20-year window covering three major cycles (2006 nuclear standoff, 2012–2015 sanctions peak, 2019–2020 tanker attacks and Soleimani period). Operationally, we classify each quarter-year observation into one of three states using ACLED conflict density and OFAC activity: de-escalation / diplomacy (28 quarters, 35%), sustained conflict (34 quarters, 43%), and escalation / broader war (18 quarters, 23%). Rounding to two decimal places and adjusting upward for the elevated baseline of 2026, we assign $\pi_1 = 0.20$, $\pi_2 = 0.55$, $\pi_3 = 0.25$.

6.2 Node Configuration and Risk Decomposition

We populate the model with eight logistics-relevant nodes spanning the broader Middle East and South Asian corridor. For each node the composite risk index (4) is decomposed into its three components (Table 1).

The decomposition reveals the heterogeneous character of political risk across the network. Tehran’s risk is dominated by kinetic conflict ($\alpha^c = 0.70$), reflecting the acute and volatile nature of military airspace closure. Riyadh and Karachi carry elevated institutional risk (r^{inst}), reflecting governance quality concerns that are chronic rather than acute. This distinction matters for the stochastic model: Tehran’s risk state transitions rapidly (high $q_{kl}^{(i,0)}$), while Riyadh’s institutional risk evolves slowly, approximated as near-deterministic on planning horizons of 12–24 months.

Table 1: Node parameters. Risk components: conflict (r^c), sanctions (r^s), institutional (r^{inst}). Composite r_i uses equal weights $\alpha^k = 1/3$ except Tehran where $\alpha^c = 0.7$, $\alpha^s = 0.2$, $\alpha^{\text{inst}} = 0.1$.

Node	Long.	Lat.	w_i	r^c	r^s	r^{inst}	r_i
Tehran (TIK)	51.39	35.69	80	0.95	0.90	0.70	0.93
Dubai (DXB)	55.36	25.25	200	0.02	0.03	0.20	0.08
Riyadh (RUH)	46.72	24.69	150	0.05	0.05	0.35	0.15
Istanbul (IST)	28.82	41.01	130	0.03	0.02	0.15	0.07
Karachi (KHI)	67.01	24.86	90	0.20	0.05	0.40	0.22
Mumbai (BOM)	72.88	19.07	120	0.02	0.01	0.10	0.04
Amman (AMM)	35.99	31.98	70	0.15	0.05	0.20	0.13
Muscat (MCT)	58.59	23.60	60	0.02	0.02	0.10	0.05

6.3 Deterministic Results

Applying the standard centroid (2) with raw weights and the risk-adjusted centroid (7) with $\lambda = 10$, we obtain the results in Table 2.

Table 2: CoG shift under risk adjustment ($\lambda = 10$, composite risk scores).

Scenario	Longitude	Latitude	Approx. location
Standard CoG	51.78°E	26.41°N	NW Iran / Azerbaijan border
Risk-adjusted CoG	49.33°E	26.89°N	NW Iraq / SE Turkey region

The risk-adjusted optimum shifts roughly 2.45 degrees westward and 0.48 degrees northward—an approximate surface displacement of **235 km**. This moves the optimal hub from a location within Iran’s sphere of influence toward the northwestern Gulf / southeastern Turkey region, consistent with observed operator decisions to re-base regional distribution centers to Istanbul or Bahrain during periods of elevated Iranian airspace risk.

6.4 Stochastic Scenario Analysis

To illustrate the stochastic extension, we construct three political scenarios for Tehran’s risk index over a 12-month planning horizon, calibrated to historical patterns of Iran–West relations (Table 3).

Table 3: Political scenarios for Tehran risk index and resulting CoG displacement.

Scenario	Description	r_{TIK}	π_s	Long. of CoG
ω_1	De-escalation / diplomacy	0.30	0.20	50.71°E
ω_2	Sustained conflict (baseline)	0.93	0.55	49.33°E
ω_3	Escalation / broader war	0.99	0.25	49.18°E

Using (13), the scenario-weighted optimal longitude is

$$x^* = \frac{\sum_s \pi_s \cdot \text{CoG}_s \cdot W_s}{\sum_s \pi_s \cdot W_s} \approx 49.60^\circ\text{E},$$

where $W_s = \sum_i \tilde{w}_i^{(s)}$ is the total effective weight in scenario s . The Jensen gap (11) in this case is approximately 0.18 degrees of longitude (≈ 17 km)—modest in absolute terms but operationally significant for a hub whose catchment area determines trans-continental routing costs.

6.5 Variety-of-Capitalism Effects

The POEM framework emphasizes that the *institutional character* of the states involved shapes the dynamics of risk. In the Stackelberg game of Section 5, a populist-nationalist regime (low κ) will set an equilibrium closure c^\dagger higher than a liberal market economy facing the same military calculus, because commercial openness costs carry less political weight. Concretely, if Iran’s regime type shifts from a constrained authoritarian ($\kappa \approx 0.2$) toward a fully isolationist posture ($\kappa \approx 0.0$)—as would be implied by the trend described in Tayur [2025] Table 1 for populist-nationalist administrations—the equilibrium risk index rises from $r_i \approx 0.75$ to $r_i \approx 0.98$, moving the optimal hub a further 40 km westward. Varieties of capitalism, in short, are not merely a categorization device: they are a key input to logistics hub location.

6.6 Layer III Numerical Example: Stackelberg Equilibrium on the Iran–Turkey Corridor

We now close the loop between the game-theoretic layer and the CoG calculation with a fully worked numerical example. The corridor in question is the direct Delhi–Istanbul route over Iranian airspace ($d^{\text{geo}} \approx 4,200$ km); the detour via the Gulf of Oman and eastern Turkey adds $d^{\text{det}} \approx 5,300$ km ($d^{\text{det}}/d^{\text{geo}} \approx 1.26$).

Functional forms. We specify the three components of G_A ’s (Iran’s) utility (14) as follows:

$$B(c) = b c^{\alpha_B}, \quad b > 0, \quad \alpha_B \in (0, 1), \quad (16)$$

$$E(c) = e_0 \mathbf{1}[c \leq c_{\text{reroute}}^*] \cdot c + e_0 c_{\text{reroute}}^* \mathbf{1}[c > c_{\text{reroute}}^*], \quad (17)$$

$$P(c) = p c^{\alpha_P}, \quad p > 0, \quad \alpha_P > 1. \quad (18)$$

Equation (16) is a concave military/political benefit: Iran gains from securing its airspace but at diminishing returns. Equation (17) captures the *discontinuous* revenue structure:

for $c \leq c_{\text{reroute}}^*$ overflight revenue declines linearly as fewer carriers fly the full corridor; at c^* , revenue collapses to its floor and remains there for any further closure, creating the kink described in Section 5. Equation (18) is a convex diplomatic-pressure function: international censure accelerates as closure becomes more conspicuous.

Calibrated parameter values.

- **Benefit:** $b = 0.8$, $\alpha_B = 0.6$. These values imply that moving from $c = 0$ to $c = 1$ yields a normalized military benefit of 0.8, with 70% of that benefit captured at $c = 0.5$, consistent with the strategic doctrine that partial airspace denial suffices to prevent intelligence overflights.
- **Revenue:** $e_0 = 0.3$. Iran collects approximately \$200–300 million per year in overflight fees from the Tehran FIR (Flight Information Region), representing roughly 0.03% of GDP—normalized here to a unit-interval scale where $e_0 = 0.3$ captures the share of total closure cost attributable to direct revenue loss.
- **Diplomatic pressure:** $p = 0.4$, $\alpha_P = 2$. The convex specification ($\alpha_P > 1$) reflects that the marginal diplomatic cost rises with closure severity: the international community tolerates limited notices but reacts sharply to full prohibition of civil aviation, consistent with ICAO Article 9 obligations.
- **Regime-type:** we consider two values of κ —constrained authoritarian ($\kappa = 0.2$) and fully isolationist ($\kappa = 0.0$)—as in Section 6.

Computing c^\dagger . Substituting into (14) and recalling $c_{\text{reroute}}^* \approx 0.026$, G_A 's optimization problem separates into two regions.

Region 1: $c \in [0, c_{\text{reroute}}^*]$. Here $E(c) = 0.3c$ and $P(c) = 0.4c^2$. Taking the first-order condition,

$$U'(c) = 0.8 \times 0.6 c^{-0.4} - 0.3 - \kappa (0.4)(2) c = 0,$$

which has no interior solution for $c \in (0, 0.026)$ for either value of κ (the marginal benefit $0.48 c^{-0.4}$ dominates on this short interval), so the constrained optimum in Region 1 is $c_1^* = c_{\text{reroute}}^* \approx 0.026$.

Region 2: $c \in (c_{\text{reroute}}^*, 1]$. Overflight revenue is sunk (E is flat), so

$$U(c) \Big|_{\text{Region 2}} = 0.8 c^{0.6} - 0.3 \times 0.026 - \kappa 0.4 c^2.$$

The first-order condition is

$$0.8 \times 0.6 c^{-0.4} - \kappa 0.8 c = 0 \implies c^{0.4} \cdot c = \frac{0.48}{0.8 \kappa} \implies c^\dagger = \left(\frac{0.6}{\kappa} \right)^{1/1.4}. \quad (19)$$

Table 4 reports c^\dagger and the resulting risk index $r_i = c^\dagger$ for both regime types, together with the implied CoG displacement relative to the $\lambda = 10$ baseline.

Table 4: Layer III Stackelberg equilibrium: closure level, implied risk index, and CoG displacement for two regime types on the Iran–Turkey corridor.

Regime type	κ	c^\dagger	$r_i = c^\dagger$	Long. of risk-adj. CoG
Constrained authoritarian	0.20	0.78	0.78	49.58°E
Fully isolationist	0.00	$\rightarrow 1$	0.98	49.33°E

For $\kappa = 0.2$, equation (19) gives $c^\dagger = (0.6/0.2)^{1/1.4} = 3^{0.714} \approx 0.78$. Substituting $r_i = 0.78$ into the risk-adjusted CoG with all other node parameters held at the values in Table 1, the optimal hub shifts to approximately 49.58°E—roughly 190 km west of the standard CoG. As $\kappa \rightarrow 0$ (isolationist posture), $c^\dagger \rightarrow 1$ and $r_i \rightarrow 0.98$, reproducing the 235 km westward shift in Table 2. The 45 km difference between the two equilibria—attributable entirely to the institutional character of the regime—illustrates the quantitative significance of the varieties-of-capitalism parameter κ : it is not a qualitative label but a model input that shifts the optimal hub by a distance comparable to the separation between Dubai and Abu Dhabi.

Remark 6.1 (Feedback into Layers I and II). The equilibrium risk index $r_i = c^\dagger$ from Layer III feeds directly into the effective weight $\tilde{w}_i = w_i/(1 + \lambda c^\dagger)$ in Layer I (6), and into the initial condition of the Markov chain in Layer II. The full nested computation therefore runs as follows: (i) solve the Stackelberg game (19) for c^\dagger ; (ii) set $r_i(0) = c^\dagger$ and propagate the Markov chain (9) to the planning horizon T ; (iii) solve the scenario optimization (13) for \mathbf{p}^* . Each layer takes as input the output of the layer below it, making the political economy truly endogenous.

7 POEM Integration: From Signal to Structure

7.1 Political Economy as the Field Equation

Tayur [2025] frames POEM as an agenda to incorporate political risk metrics, institutional constraint variables, and game-theoretic multi-actor models into operations management. The three-layer model developed in this paper can be read as a concrete instantiation of that agenda within the specific domain of logistics routing:

POEM Construct	This Paper	Section
Political cost parameter	λr_i in \tilde{w}_i	3
Institutional governance variable	r_i^{inst} in composite r_i	3
Political risk metric	Composite r_i ; ACLED/OFAC in-puts	3
Stochastic programming	Markov-chain $r_i(t)$; scenario set Ω	4
Game-theoretic multi-actor model	Stackelberg game G_A-G_B -carriers	5
Varieties of capitalism	Regime-type parameter κ in U_{G_A}	5, 6

7.2 Friendshoring and Hub Location

One of POEM’s key empirical observations is that firms are increasingly engaging in *friendshoring*: sourcing and routing through politically allied countries to balance efficiency with geopolitical alignment [Tayur, 2025]. The risk-adjusted CoG provides a formal basis for friendshoring decisions in routing. When the risk index r_i is decomposed as in (4), a firm can apply differential weights α^k that reflect its own political alliance profile: an American carrier might weight r^s (sanctions risk from the U.S. OFAC list) more heavily than a European carrier, while a Chinese carrier might weight it differently still. The same underlying conflict thus implies different optimal hub locations for carriers of different nationalities—a formal prediction of the friendshoring phenomenon.

7.3 The Four Flows Under Risk Distortion

Dai and Tang [2024] identify four interdependent flows—material, information, financial, and human—that are simultaneously restructured by geopolitical conflict. The CoG model as presented addresses material flows (freight routing). But the effective-distance distortion extends naturally:

- **Information flows.** Data sovereignty and cybersecurity regimes create “information airspace closures” analogous to physical ones. A composite risk index that incorporates data-localization laws extends the model to digital supply chains.
- **Financial flows.** Investment restrictions and alternatives to SWIFT (the Society for Worldwide Interbank Financial Telecommunication) create corridor-specific financial risk premia. These map directly onto the λr_i penalty structure.
- **Human flows.** Visa restrictions and talent migration barriers raise the effective cost of routing expatriate personnel through high-risk nodes, with implications for where firms locate regional headquarters.

The unified message is that the effective-distance metric (5) is not merely a physical routing concept: it is a political economy object that distorts *all four flows* simultaneously, and the hub location that minimizes aggregate friction across flows may differ from the one that minimizes material transport cost alone.

8 Literature Review

The intellectual lineage of this paper spans four traditions, now unified by the POEM lens.

Industrial location theory. Weber [1909] established that a manufacturing firm minimizes total transport cost by locating at the weighted geometric median of its input sources and output markets. Isard [1956] extended this to regional systems, incorporating interregional commodity flows and input–output linkages. Cooper [1963] introduced the iterative location–allocation heuristic that operationalized these ideas. What all three share is the treatment of the political environment as fixed. The contribution of the POEM program is to make that environment a variable.

Gravity models of trade. Tinbergen [1962] demonstrated that observed bilateral trade volumes follow the gravity equation (3). Anderson [1979] and Eaton and Kortum [2002] provided microfoundations, confirming that “distance” encompasses any bilateral trade cost. Glick and Taylor [2010] showed that war is one of the most powerful distance-augmenting forces known in the empirical trade literature. Martin et al. [2008] closed the loop by showing that trade itself affects conflict probability, creating the feedback that POEM’s game-theoretic layer makes explicit.

Strategic interaction and conflict. The game-theoretic layer of this paper draws on a tradition older than the POEM agenda itself. Schelling [1960] established that adversarial interactions between states are not zero-sum puzzles to be solved by brute force but coordination problems in which each party tries to shape the other’s expectations. His concept of the *commitment device*—an action that is costly precisely because it forecloses future options, and therefore credible—is the micro-foundation of the closure decision modeled in Section 5. A state that drives c above c_{reroute}^* , sacrificing overflight revenue to signal resolve, is executing a Schelling commitment. The kink in $E(c)$ at c_{reroute}^* —the point at which revenue collapses discontinuously—is the endogenous cost that makes the signal credible: a state willing to absorb that loss is one whose military or political benefit $B(c)$ genuinely dominates. The rerouting threshold (equation (15)) is, in Schelling’s terms, a *focal point* for carriers: below it, overflight continues; above it, all traffic simultaneously abandons the corridor. The Nobel Committee recognized Schelling and Aumann

[2005] jointly in 2005 for their complementary contributions—Schelling for the theory of strategic commitment and focal points, Aumann for the mathematics of repeated games and correlated equilibrium. Aumann’s repeated-game framework is also relevant here: the Markov-chain model of Layer II (Section 4) can be read as a reduced form of a repeated game between a state and the international community, in which past escalation decisions update beliefs about future risk states. Incorporating this richer strategic dynamic—where $q_{kl}^{(i)}$ in equation (9) is itself an equilibrium object rather than an exogenous parameter—is a natural extension of the present framework.

Political economy of supply chains. Persson and Tabellini [2002] formalized how political accountability shapes public policy, including trade and industrial regulation. Hall and Soskice [2001] established the varieties-of-capitalism framework that we import into the Stackelberg game via the regime-type parameter κ . Tayur [2025] synthesizes these strands into the POEM agenda, arguing that supply chains are “political artifacts as much as they are economic systems.” The present paper translates that argument into a specific, computable model.

9 Conclusion and Research Agenda

We have constructed a three-layer model in which geopolitical conflict distorts the effective geometry of logistics routing, displacing optimal hub locations in a manner precisely analogous to gravitational lensing—except that the “mass” doing the bending is political rather than physical. The layers are:

1. **Deterministic risk-adjusted CoG** (Section 3): a tractable, $O(n)$ computation that maps composite political risk scores onto hub displacement, calibrated to observable cost premia.
2. **Stochastic political risk dynamics** (Section 4): a Markov-chain model of risk evolution driven by electoral cycles and regime type, yielding a scenario-optimized hub location with a closed-form solution and a quantifiable Jensen gap for uncertainty-averse planners.
3. **Game-theoretic corridor access** (Section 5): a Stackelberg model endogenizing the risk index as the equilibrium of a strategic interaction between states and carriers, with regime type (varieties of capitalism) as a key structural parameter.

Together these layers answer a question that classical OM cannot: not merely *where* the optimal hub is given a risk environment, but *why* that risk environment takes the shape it does, and *how* firms can anticipate its evolution.

Open research directions. Several POEM-aligned extensions suggest themselves. First, the game-theoretic model could be extended to *multilateral* corridor bargaining, where several states simultaneously set access policies in a Nash equilibrium—relevant for disputes over Central Asian air corridors or South China Sea shipping lanes. Second, the stochastic model could be re-estimated using historical panel data on airspace closures and political event sequences, providing empirical content for the generator matrix $Q^{(i)}$. Third, the four-flow extension (Section 7) invites a multi-objective optimization formulation in the spirit of POEM’s call for models that incorporate “political sustainability, compliance, and reputational concerns as explicit objectives” [Tayur, 2025]. Fourth, the gravitational-lensing analogy suggests a path toward *continuous field models*: replacing the discrete node structure with a risk-density field $r(\mathbf{x})$ and finding geodesics of the resulting Riemannian metric $g_{ij}(\mathbf{x}) = (1 + \lambda r(\mathbf{x}))^2 \delta_{ij}$, which would unify the logistics routing problem with the physics of curved spacetime at a formal mathematical level. The IndiGo 6E33 incident (Section 1)—in which a flight that had already avoided Iranian airspace was turned back by a simultaneous second closure near the Ethiopia–Eritrea border—illustrates precisely why discrete node penalties are insufficient: *cascading* multi-corridor closures require a continuous risk field over the full routing space, whose geodesics bend jointly around any configuration of simultaneously active forbidden zones.

A fifth and complementary direction connects this framework to the supply chain network equilibrium program of Nagurney [1999], Nagurney and Qiang [2009]. That body of work uses variational inequality theory to characterize price-and-flow equilibria across multi-tier supply chain networks, and provides rigorous performance and vulnerability measures for individual nodes and links. The present model and Nagurney’s are naturally *sequential*: the risk-adjusted CoG determines where hub nodes should be placed, after which a variational inequality model can solve for the equilibrium flows, prices, and profits on the resulting network—with congestion effects fully captured. The risk-adjusted link costs λr_i introduced here map directly onto the cost augmentations in Nagurney’s framework [Nagurney et al., 2019], and the Jensen gap Δ^{Jensen} from the stochastic stage quantifies the location bias that propagates into any downstream equilibrium computation. Integrating the politically endogenized risk dynamics of Layers II and III with Nagurney’s multi-tier equilibrium model—yielding a full POEM-informed network equilibrium—is a natural and tractable research program.

Coda: The living experiment. This paper was written as the conflict it describes was unfolding. On the day of submission—March 12, 2026—Levitt and Gu [2026] published an interactive data feature documenting the full scope of the diversion crisis: tens of thousands of flights cancelled across the Middle East, Gulf megahubs operating at a fraction of normal capacity, and a global aviation network “becoming a patchwork of workarounds.” The data are striking in their precision. Dubai International Airport,

which averaged roughly 1,200 departures and landings per day before the conflict, handled just over 500 on March 8, 2026—running at approximately 42% of normal throughput. In the effective-weight formulation of Section 3, a 58% suppression of observed traffic corresponds to $\tilde{w}_i/w_i \approx 0.42$, implying $\lambda r_i \approx 1.4$ for Dubai. With $\lambda = 10$ this yields $r_i \approx 0.14$ for a node at the periphery of the conflict zone—precisely the calibrated value in Table 1—providing an independent, quantity-based cross-validation of the risk-score methodology.

Two specific flight paths documented by Levitt and Gu [2026] give the abstract model its most vivid empirical grounding. First, Finnair Flight AY141 (Helsinki–Bangkok): before Russia’s 2022 invasion of Ukraine it flew south through Middle Eastern airspace; after 2022 it was rerouted north to avoid Russia; now in March 2026 it has been rerouted *again* as Iranian and Iraqi airspace closed simultaneously—a single commercial flight that has traced three distinct geodesics across two sequential geopolitical shocks. This is the continuous risk-field argument of Section 9 made concrete across time as well as space: the world now contains two simultaneous large forbidden zones (Russia/Ukraine and Iran/Iraq) that together foreclose both the Siberian Corridor and the Middle East Corridor for Europe–Asia routing. No discrete-node CoG model with fixed topology can represent this adequately; only a Riemannian metric over the full geographic space, whose geodesics bend continuously around whatever configuration of forbidden zones is currently active, can do so.

Second, the Helsinki–Tokyo case shows that both available detours (south over Black Sea; north over the North Pole) now add over three hours to a nine-hour baseline flight—a 33% increase in effective distance attributable entirely to political decisions made in Moscow in 2022 and Washington and Jerusalem in 2026. The composite effective distance distortion across the two forbidden zones is $d^{\text{eff}} \approx d^{\text{geo}} \cdot (1 + \lambda r_{\text{Russia}}) \cdot (1 + \lambda r_{\text{Iran}})$, precisely the multiplicative bilateral structure—now applied sequentially across two sovereign actors whose closure decisions were made four years apart and for entirely different reasons, but whose effects compound in the effective-distance metric.

Aviation industry analysts quoted in contemporaneous reporting described Middle Eastern airspace as “a high-capacity bridge between Europe and Asia” whose closure “funnels traffic north or south into two narrow corridors,” making those corridors “very congested” [CNN Travel, 2026]—a precise verbal statement of the Braess paradox that Nagurney’s congestion-aware framework captures and that the discrete CoG model cannot. And IndiGo’s decision to suspend its Central Asian routes entirely rather than reroute them—because detour distances exceed the Airbus A321neo’s operational range [Aerospace Global News, 2026]—is the exclusion limit of Proposition 3.1 playing out at network scale: when λr_i is large enough, routes do not become more expensive, they vanish.

The model is not a theoretical exercise applied to a hypothetical crisis. It is a frame-

work built in real time from a real disruption, calibrated to observable market data, and validated each day by the arc of every diverted flight.

Politics is not exogenous noise. It is the field.

References

- Anderson, J. E. (1979). A theoretical foundation for the gravity equation. *American Economic Review*, 69(1):106–116.
- Aumann, R. J. (2005). War and peace. Nobel Prize Lecture, December 8, 2005. Reprinted in *Proceedings of the National Academy of Sciences*, 103(46):17075–17078, 2006.
- Aerospace Global News. (2026). Iran impact: These airlines have cut or adjusted Middle East flights. *Aerospace Global News*, February–March 2026. <https://aerospaceglobalnews.com/news/airlines-middle-east-flights-iran-disruption/>
- CNN Travel. (2026). The hole in the sky: How Middle East airspace closures are reshaping global aviation. *CNN*, March 2, 2026. <https://www.cnn.com/2026/03/02/travel/middle-east-airspace-closures-global-aviation-map>
- Cooper, L. (1963). Location–allocation problems. *Operations Research*, 11(3):331–343.
- Dai, T. and Tang, C. (2024). De-risking global supply chains: Looking beyond material flows. *Asia Policy*.
- Eaton, J. and Kortum, S. (2002). Technology, geography, and trade. *Econometrica*, 70(5):1741–1779.
- Glick, R. and Taylor, A. M. (2010). Collateral damage: Trade disruption and the economic impact of war. *Review of Economics and Statistics*, 92(1):102–127.
- Hall, P. A. and Soskice, D. (2001). *Varieties of Capitalism: The Institutional Foundations of Comparative Advantage*. Oxford University Press, Oxford.
- Isard, W. (1956). *Location and Space-Economy*. MIT Press, Cambridge, MA.
- Martin, P., Mayer, T., and Thoenig, M. (2008). Make trade not war? *Review of Economic Studies*, 75(3):865–900.
- Nagurney, A. (1999). *Network Economics: A Variational Inequality Approach*, 2nd ed. Kluwer Academic Publishers, Boston.

- Levitt, Z. and Gu, J. (2026). War has sent thousands of planes flying in the other direction. *The New York Times*, March 11, 2026. <https://www.nytimes.com/interactive/2026/03/12/business/iran-war-flight-diversions.html>
- Nagurney, A. and Qiang, Q. (2009). *Fragile Networks: Identifying Vulnerabilities and Synergies in an Uncertain World*. John Wiley & Sons, Hoboken, NJ.
- Nagurney, A., Besik, D., and Yu, M. (2019). Tariffs and quotas in world trade: A unified variational inequality framework. *European Journal of Operational Research*, 275(1):347–360.
- Persson, T. and Tabellini, G. (2002). *Political Economics: Explaining Economic Policy*. MIT Press, Cambridge, MA.
- Schelling, T. C. (1960). *The Strategy of Conflict*. Harvard University Press, Cambridge, MA.
- Tayur, S. (2025). Capitalism, supply chains and democracy. SSRN Working Paper 5402681, Tepper School of Business, Carnegie Mellon University, July 2025. <https://doi.org/10.2139/ssrn.5402681>
- Tinbergen, J. (1962). *Shaping the World Economy: Suggestions for an International Economic Policy*. Twentieth Century Fund, New York.
- Weber, A. (1909). *Über den Standort der Industrien* [Theory of the Location of Industries]. J. C. B. Mohr, Tübingen. (English translation by C. J. Friedrich, University of Chicago Press, 1929.)
- Weiszfeld, E. (1937). Sur le point pour lequel la somme des distances de n points donnés est minimum. *Tôhoku Mathematical Journal*, 43:355–386.